

Machining parameter investigation of Ti-6Al-4V alloy on milling process with Al₂O₃ Nano hybrid cutting fluid

C. Manivel^{a,*}, P. Siva^b, S.M. Vijayarajan^c, and M. Ameena Banu^d

^aAssistant Professor, Department of Mechanical Engineering, NPR College of Engineering & Technology, Natham, Dindigul, Tamilnadu, India - 624401

^bAssistant Professor, Department of Mechanical Engineering, JCT College of Engineering and Technology, Pichanur, Coimbatore, Tamilnadu, India - 641105

^cAssociate Professor, Department of Electronics & Communication Engineering, NPR College of Engineering & Technology, Natham, Dindigul, Tamilnadu, India - 624401

^dProfessor, Department of Electronics & Communication Engineering, NPR College of Engineering & Technology, Natham, Dindigul, Tamilnadu, India - 624401

The Ti6Al4V alloy was difficult to cut material because of its inherent properties, however greater application in extreme operating conditions; hence, the impact of machining parameters on nanoparticle diffused cutting fluids study was essential. The aim of this work was to examine the impact of alumina (Al₂O₃) nano-diffused cutting fluids under the minimal quantity lubrication (MQL) approach in the milling process on Ti6Al4V Alloy. Nano-based cutting fluid was prepared in unique weight percentage concentrations of 0%, 1%, and 2% of nanoparticles with base fluid. The experiments were conducted to analyse the effect of spindle speed, cutting feed and axial cutting depth on the concentration of nanoparticles using the face-centred composite design (CCD) on cutting tool temperature (Ct) and surface roughness (Ra). The results revealed that Alumina nanofluid minimizes the Cutting tool temperature and enhances the surface roughness (Ra). The responses were optimized using the desirability function based analysis (DFA) for nano based cutting fluids. The optimal process parameters of the Al₂O₃ nanofluid weight percentage concentration of nanoparticles were (2%), cutting feed (0.142 mm/rev), spindle speed (104 m/min) and DOC (0.5 mm).

Keywords: Nano particle, Hybrid cutting fluid, Alumina, ANOVA, RSM, DFA

Introduction

Various studies have recently focused on the sustainable production process to improve product quality. Milling is the material removal process suitable for mass production [1, 2]. The point of contact of the cutter on the material is larger than in other machining processes, which is why it is called the multipoint cutter [3]. Because of the high machining costs and low productivity of harder machining materials like titanium and its alloys, numerous applications are concerned with achieving surface integrity, quality, and size [4]. Titanium is a widely used material due to its fabulous material properties such as corrosion, light material, height-to-weight ratio and high temperature etc., the preliminary alloy Ti6Al4V observed through the microstructure which is its phase α stabilizer contains Aluminum 6% and its β phase contains vanadium 4% [4, 5]. Normally, the feed rate, spindle speed and DOC are the basic

conventional machining parameters, among which speed is the crucial element to estimate the production rate and its quality. Therefore, for machining hard materials like titanium alloys industrial coolants (i.e., mixed coolant with nanoparticles) is introduced during machining to minimize the dispersal of heat at the tool-chip contact [5, 6].

Industrial coolant oil has a significant part in estimating the performance of the response of material. commonly cutting fluid embrace oil, water-primarily based emulsion gel, pastes etc., a lot of the usage of industrial coolant and its effects on environmental and human health is that one the important considerable factor in all aspects particularly in manufacturing sectors like automobile, aerospace, paramedical and materials manufacturing industries [7, 8]. There's more investigation occurring about green manufacturing in machining industries. The mechanism of this reduces the environmental heaps to provide a smart surface finish product. The choice of machining parameter and supply of cutting fluid to decrease the temperature in the cutting region is an extremely essential one for harder materials. In recent trends the utilization of nanoparticles diffused cutting

*Corresponding author:
Tel : +91-98420 59997
E-mail: manivelcc@gmail.com

fluid is one of the answers to achieving a high rate of heat exchange in the cutting zone [9, 10].

The integration of nano reinforced with cutting oil such as Alumina, metal disulphide, oxide of silicon dioxide and diamond etc., provided higher lubrication and cooling results at the cutting edge throughout machining. Since it created an adhere effect of machining the adding of diffused nano additives with agent or base fluid to make better performance on the machining surfaces additionally it leads to reducing the temperature at the cutting point [10]. The dry machining method is appropriate for forged iron and a few classes of brass material to minimize the requirement of metal working fluid, despite the fact that during machining, there are issues with poor surface quality and significant tool wear. The improved cutting fluid methodology of mist sprayed on machining zone techniques used some preliminary studies and ensuing that have not fully reduced cooling on the cutting zone [11]. To prevent overheating during Ti6Al4V machining, flood cooling is a common cooling technique used in the engineering sector. This is done in order to seek further studies to increase the machinability to achieve property manufacturing. Using overflow coolant leads to health and environmental problems that require finding entirely new solutions [11, 12]. To improve surface integrity, machining quality, and manufacturing quality, new environmentally friendly cooling and lubrication systems must be implemented. [12]. There are many lubrication techniques that adore dry machining, MQL cryogenic etc., for environmental eco-friendliness. Improved stiffness, hardness, high strength, superior thermophysical phenomena, and wear resistance are all achieved with the use of nanoparticles. When compared to basic lubricants with superior heat dissipation capabilities, this enhances and measures thermal conductivity [13, 14]. The studies provided above reveal that nano-cutting fluids have demonstrated favorable feedback on the behavior of machining performance in a variety of machining operations, including drilling, grinding, milling, and turning. MQL nano-cutting fluid is one of the methods that are advised for optimum wettability, conduction, and convection aspects at the lowest possible consumption [14, 15].

The usage of nano cutting fluids and their effects on machining behavior and attributes have been discussed on multiple occasions; the findings have primarily focused on the decrease of heat, tool wear, and cutting forces. Among the most widely used nano additives are Al_2O_3 nanoparticles, which have mechanical, tribological, and thermal properties [16-18]. Few research, meanwhile, have looked at its consequences in various processing scenarios. The literature assessment also revealed a research deficit in the area of studying the impacts of nanofluids in titanium alloy machining.

According to the literature, alumina worked well as a nano addition in conventional cutting oil; however, certain investigations have shown that it has an impact on

different control operations. Alumina nano additive has superior properties such as wear resistance, conductivity, hardness, phase stability and good dimensional stability. Regression equations and three dimensional (3D) surface plots were created to measure the responses under flood cooling/grinding lubrication conditions of the Ti6Al4V alloy [19].

The literature indicates that coolants based on nanotechnology have little effect on titanium alloy machining. The advanced design of experiments (DOE) method was used to determine the ideal parameters for improved surface attributes. The potent DOE method was designed to reduce the amount of tests and repetitions. In engineering applications, Box-Bohen (BBD), Taguchi, and Central Composite Design (CCD) are frequently utilized. These techniques make for an economical experimental setup. Recent years have seen the application of metaheuristic algorithms for a variety of engineering and machining challenges, including Genetic Algorithm (GA), Simulated Annealing (SA), and Particle Swarm Optimization (PSO). Processing parameter optimization by Design of Experiments (DOE) using metaheuristic algorithms has also gained popularity.

These research gaps were found from the open-ended literature evaluation.

(i) No work has been reported using Servo 'S' cutting oil and distilled water as the base fluid.

(ii) There is no detailed milling work using nanofluid and the MQL technique to optimize cutting parameters by assessing the desire function for the weight percentage by weight of nanoparticles as an input. Instead, constrained work was taken into consideration when milling Ti6Al4V alloy using dry machining.

(iii) Although Ti6Al4V is widely utilized in many different applications, there isn't much literature available to discover how machining parameters and Al_2O_3 nanofluids affect the weight percentage responses of nanoparticles employed as inputs.

Methodology

Nano cutting fluid cost, dispersion and stability, tool use and maintenance, and environmental impact are some of the challenges identified in the literature. This can be solved with most adherents; this study carefully considered the preparation of the cutting fluid and its stable analysis during periods of time suitable for the processing conditions. The ultimate objective of the study was to experiment the effects of aluminum oxide nanoparticles dispersed in the base fluid with Servo S cutting oil during Ti6Al4V machining. The experimental and analysis study was minimizing the cutting temperature at the shear point and minimizing the surface roughness on the material surface. To reduce the temperature and preserve acceptable surface quality, it is a significant machining task to research the machining of Ti6Al4V alloys from the beginning. To

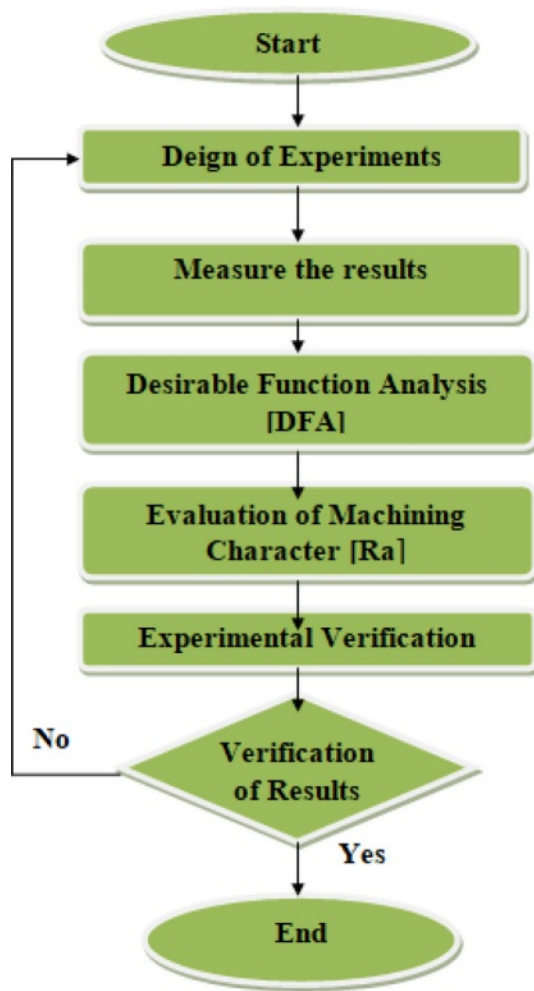


Fig. 1. Experimentation methodology.

reduce the heat at the machining point that conventional high pressure hybrid cutting oil passes under flooded conditions. The cutting oil used causes the adverse effect of the cutting oil in conventional machining. Therefore, adding nanoparticles to base fluid or traditional cutting oil acted as a superior lubricant that improves thermal

conductivity and lowers temperature [20]. Since the Ti6Al4V alloy is a more difficult material to machine and the cutting fluid is a consideration, it makes sense to do some work to develop and observe long-life cutting oils. This study was conducted to estimate the efficiency of machining titanium alloys under alumina nano based cutting oil with lubricating conditions for optimal cutting parameters [20, 21]. To this attainment, several combinatorial input parameters were considered. Experimental design software of Design Expert was used to find and minimum count of repeated experimentations, input parameters and the RSM approach was adjusted to optimize the editing process several optimization problems [22]. The Experimentation work process of flow chart shown in Fig. 1.

Materials and Methods

Cutting fluid preparation method

A two-step process has been proposed for preparing nanometric cutting oil. First, the required amount of aluminum oxide nanoparticles and sodium dodecylbenzene sulfonate (SDBS) surfactant is measured using a digital balance with a high-precision strain gauge sensor system (Servo brand SF400) with an accuracy of 0.1 g for mixture rule formulas, refer Equation (1). Sodium dodecylbenzene sulfonate is an ionic surfactant (SDBS). Serves as a surfactant in cyclophane's ionic self-assembly process. It has been used to stabilize graphene nanoflake dispersion during liquid phase preparation [23]. It can also produce well-resolved spectral characteristics and sustain individual nanotubes in aqueous media. C. Yang et.al. The measured viscosities of Al₂O₃ (80 nm) and deionized water (DIW)-based nanofluids were also found to increase by nearly 82% for the maximum volumetric loading of 5% nanoparticles. A similar increment (86%) of the effective viscosity of Al₂O₃ (28 nm)/distilled water-based nanofluids was also observed by Wang et al. Servo S cut oil has been selected from industrial coolant and deionized water as the base fluid, which is referred to as standard metalworking fluid. Alumina nanoparticles



Fig. 2. Preparation of Cutting fluid by stirrer.

Table 1. Nano fluid characterization.

Characteristic	Nano Fluids	Normal Fluid
Nano-additives	Carbon tube	Soluble / emulsifiable oil
Base fluid	water-based oil, organic liquids, vegetable oil and polymeric solutions	Oil-based or straight oil
Other additives	No surfactants added	Synthetic
Scale	percentage of weight concentration	Flash

Table 2. Different sample level of cutting fluid.

No	S1	S2	S3
1.	Deionized water - 95 ml + 'S' servo cut oil - 5 ml	Deionized water - 95 ml + 'S' servo cut oil - 5 ml + 1 wt% of Alumina	Deionized water - 95 ml + 'S' servo cut oil - 5 ml + 2 wt% of Alumina

were measured and dispersed with the designed base liquid less than 100 nm. The colloidal suspension is applied to obtain nanofluids since Al₂O₃ nanoparticles are insoluble in oil or deionized water [24].

$$\text{Concentration of weight \%} = \frac{\text{The base fluid} + (\text{Nano additive weight}/\text{Nano additive weight})}{1} \quad (1)$$

First mix the tenside together with the emulsified liquid normally immiscible fluid (see Table 2) about 15 minutes later with a magnetic stirrer, add nanoparticles and stir for about 30 minutes. After that, it was exposed to ultrasonication for 90 minutes at 50 kHz and 80 W using an Ultrasonicator vibrating equipment to ensure that the nanoparticles and base liquid were distributed uniformly. It is claimed that adding surfactants to nanofluid manufacturing improves dispersion and inhibits particle agglomeration [25, 26]. The above procedure was repeated until a uniform colloidal dispersion was obtained. Fig. 2 shows the method of nano cutting fluid preparation.

For sample preparation deionized water 95 ml and

'S' servo cut oil 5 ml was used as base fluid for cutting oil. The gamma category of alumina nano powder with 99.5 plus percentage purity and 18 nm sized, hydrophilic nano powder was mixed base fluid. The FESEM image of Alumina (Al₂O₃) for 100 nm is indicated in Fig. 4.

Three different samples of cutting oils were produced for machining lubrication and shown in the illustrations. The sample preparation of the cutting fluid for 100 ml of dispersed nanoparticles [27] is shown in the Table 4 and refer Fig. 3.

The stability analysis of nano based cutting fluids affects the thermo physical properties of cutting fluids, hence stability research was crucial. The specification of Al₂O₃ nanoparticle and its pH level is shown in Table 3. The characterization of Al₂O₃ nano particle is shown in Table 4. In this study, the sedimentation of nanofluids was observed by photographing test with a camera image. The cutting fluid sample images were observed and recorded periodically for sedimentation test. (Refer Fig. 3). The disadvantage of this method was the long observation time to detect the sedimentation of particles.



Fig. 3. Cutting fluid for 100 ml sample.

Table 3. Specifications of Al₂O₃ nanoparticles.

pH Level	Particle size-Original	Solvent	Iorn	Assay Al ₂ O ₃	Arsenic	Pb
6-8	≤20 nm	80% of water	≤3 ppm	≥20%	≤2 ppm	≤10 ppm

Table 4. Al₂O₃ nanoparticles Characterization.

Properties	Values
Formula	Al ₂ O ₃
Mass	101.95 g/mol
Density	3.94 g/ml
Hardness	1700-2000
Structure	Spherical
Particle Size	13 nm
Weight Atomic	101.96 g/mol
Melting Point	2080 °c
Thermal Conductivity	36 W/m.K

Experimental Setup and Procedure

Biomedical compatibility and increased demand in the medical field made Ti-6Al-4V a suitable candidate for human parts because of their superior mechanical properties [1, 11, 28]. The Design of Experiments Response Surface methodology (RSM) was used as the basis for conducting experiments in this study. Design Expert software version 11 was used to create the experiment.

The experimental table was created from the central composite face-centred design (CCD) with not exceeding the different ranges of machining parameters given in Table 5. The cutting parameters depend on the following factors, such as the diameter of the cutting edges of the knife, the number of cutting edges of the tool, the shape of the cutting edges of the knife, the material to be cut, the desired surface finish and the desired accuracy. All these parameters and factors determine the size of the chip removed from the material.

The size of the chip depends mainly on the feed rate,

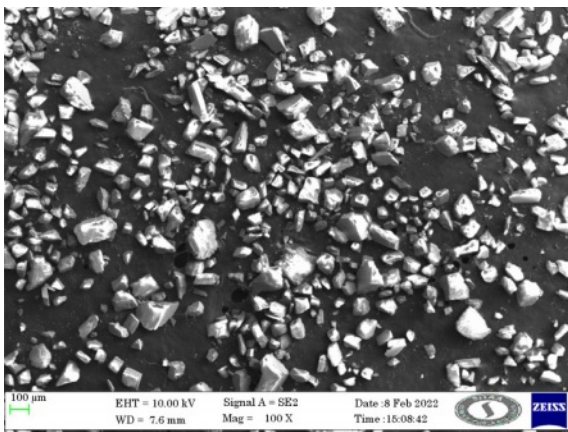


Fig. 4. FESEM image of Alumina (Al₂O₃) for 100 nm.

Table 5. Machining parameters limit level.

Parameters with Units	Label	Low	Medium	High
Spindle speed (m/min)	A	80	120	160
Feed rate (mm/rev)	B	0.08	0.14	0.2
DOC (mm)	C	0.5	1	1.5
Alumina concentration (Nanoparticles) wt%	D	0	1	2



Fig. 5. Experimental Setup with temperature and surface measurement.

Table 6. Experimental Data's for Ti-Al-4V Alloy.

Experiment Number	A: Spindle speed (m/min)	B: Feed rate (mm/rev)	C: Axial depth of cut /DOC (mm)	D: Alumina concentration -Nanoparticles (wt%)	Cutting Temperature (°C)	Surface Roughness (µm)
1	120	0.14	1	1	526	0.92
2	80	0.08	1.5	0	455	1.3
3	120	0.08	1	1	514	1.42
4	160	0.2	1.5	0	616	1.19
5	80	0.2	1.5	2	444	1.34
6	80	0.08	0.5	0	467	1.43
7	120	0.14	1.5	1	545	1.22
8	120	0.2	1	1	594	1.19
9	80	0.2	0.5	2	431	1.1
10	120	0.14	1	0	616	1.24
11	160	0.08	0.5	2	544	1
12	120	0.14	0.5	1	508	0.83
13	120	0.14	1	1	514	0.96
14	120	0.14	1	2	525	0.58
15	80	0.14	1	1	461	1.09
16	120	0.14	1	1	539	0.99
17	160	0.2	0.5	0	607	0.79
18	120	0.14	1	1	549	0.69
19	120	0.14	1	1	534	0.98
20	160	0.08	1.5	2	626	1.23
21	160	0.14	1	1	596	0.66

the number of cutting edges and the spindle speed. However, the actual chip that the machine can remove depends on the power of the machine, material hardness, blade diameter, number of cutting edges, blade sharpness and depth per drive. Chip size can be reduced by doing one of the following, i.e. increasing the spindle speed, decreasing the feed rate, increasing the number of cutting edges. Reversing these steps increases the size of the chip. Ultimately, the chip size, feed rate, and spindle speed determine the final result of the sawing process. By increasing the spindle speed (rpm) or decreasing the feed rate, the quality of the finished cut is improved. But at the same time, the friction between the tool and the workpiece also increases. As a result, there are signs of overheating and the longevity of the tool is compromised. The rectangular Ti6Al4V alloy workpiece length 150 mm, 100 mm wide and 30 mm thick size were selected to perform the machining operation using a Haas VF 3-axis vertical CNC machine and radius end mill (MSXH440R). The roughness value read on the milled surface was measured with the surface roughness meter (SJ210). The cut-out temperature measuring device (Thermocouple temperature type TEL969001 K) was used to measure the cut-out temperature.

Measurement of cutting temperature and Surface Finish

It was evident that the nano cutting fluids in the lubrication technique results reduce cutting tool temperature than other machining under blood conditions. The MQL nanofluid forms a thin film in the tool shear point and the base coolant quickly evaporates leaving behind a tribological thin film of nanoparticles in the machining point [28]. This vanishing quickly removes temperature from the cutting point, resulting in a minimizing temperature in the machining point. Moreover, part of the heat from the material's surface is dispersed by the highly pressured mist [29]. In addition, chips are extracted from the tool tip fast, reducing friction at the cutting tool point and avoiding an increase in tool temperature brought on by the chips' presence in the cutting zone. Thin coating forms in the region of the surface of the nanoparticles. This formation of layer helps increase Brownian action within the base cutting oil. Brownian action leads to some degree of grouping of particles devoid of forming agglomerations. The particle clusters quickly transfer temperature away from the processing area, thereby improving thermal conductivity [30].

The milling temperature parameter has a significant

impact on the part's surface finishing and material removal performance. Lowering cutting temperatures can enhance milling performance by improving surface integrity [29, 30]. The temperature measurement method was used to measure the milling temperature under lubricated conditions with various machining parameters shown in Fig. 3(c).

The temperature measurement strategy is shown in the figure. A K-type thermocouple with a diameter of roughly 0.20 mm was placed under the component to monitor the surface temperature. For every experiment, the cutting temperature is determined by taking the highest temperature recorded during the milling process. The work surface's roughness is a key indicator of the superb features of the machined surface, and a workpiece's improved service efficiency can be achieved by minimizing surface irregularity. Consequently, a reduced surface roughness value is desired [24, 25].

Response surface methodology

RSM is used to analyze complex responses to certain control variables. The actual parameters of a response must be obtained empirically [26]. The Response Surface Method (RSM) is a useful technique for identifying the responses' effective control variable [31]. The highest degree polynomial should be used to develop an approximation function for the correct answer. Additionally, correlations between actual variables that

are not allowed in a conventional experimental design are examined. Furthermore, not many experiments have the benefit of a suitable experimental design for data collection. In contrast to the traditional experimental design, which is one variable at a time (OVAT), the use of graphically displayed data analysis methods Oehlert et al. (2000) was implemented and assessed at all levels of combinations [32]. Another benefit of this design style is that it enhances the models mathematics. The best parameters for machining speed, feed rate, cut depth, and alumina nanoparticle concentration were found in this study using RSM-based center front composite design (CCD) [29]. Box and Behnken et al. (1960) the CCD were best for determine the best fitting curve as a second order model. The insignificant factors are removed one variable at a time by backward linear regression process [33, 34]. ANOVA was carried for surface irregularities and tool temperature to confirm the model competence and to find out the significant factor effecting. Equations (2-3) provide the experimental readings from which the regression equation was derived. The relationship between the input and output data was deciphered and the ideal parameters were predicted using the regression equation.

Statistical Analysis

Using Design Expert software, the ANOVA, R², and regression equation for surface imperfections and

Table 7. ANOVA results for Cutting Temperature (CT).

Source	SS	dof	MS	F-value	P-value	Significant Level	% of Contribution
Model	69891.57	14	4992.25	18.12	0.0009	Significant	100
A-Cutting speed	9112.50	1	9112.50	33.08	0.0012		13.04
B-Cutting feed	3200.00	1	3200.00	11.62	0.0144		4.58
C-Axial depth of cut	1664.10	1	1664.10	6.04	0.0493		2.38
D-Nanoparticles Al ₂ O ₃ concentration	4140.50	1	4140.50	15.03	0.0082		5.92
AB	1742.40	1	1742.40	6.32	0.0456		2.49
AC	1012.50	1	1012.50	3.68	0.1037		1.45
AD	2464.90	1	2464.90	8.95	0.0243		3.53
BC	288.00	1	288.00	1.05	0.3460		0.41
BD	78.40	1	78.40	0.2846	0.6129		0.11
CD	1200.50	1	1200.50	4.36	0.0819		1.72
A ²	1052.93	1	1052.93	3.82	0.0984		1.51
B ²	68.79	1	68.79	0.2497	0.6351		0.10
C ²	1270.52	1	1270.52	4.61	0.0754		1.82
D ²	1201.12	1	1201.12	4.36	0.0818		1.72
Residual	1653.00	6	275.50				
Lack of Fit	951.80	2	475.90	2.71	0.1799	Insignificant	
Pure Error	701.20	4	175.30				
Cor Total	71544.57	20					

cutting temperature were calculated. The percentages of the input parameters' contributions were examined using the ANOVA. The F-statistic values for cutting speed (33.08), cutting feed (11.62), axial depth of cut (6.04), and alumina concentration (15.03) showed that cutting speed had the greatest influence on cutting temperature. The percentages that contribute to machining speed, feed rate, axial depth of cut, and weight percentage concentration are 13.04%, 4.58%, 2.38%, and 5.92%, in that order. A strong correlation was found between the experimental and projected cutting conditions, as indicated by the cutting temperature R² value of 97%. The higher the R² score, the more accurate the model was. The minimal error occurrence of the expected analysis is displayed in the predicted versus experimental figures.

$$\begin{aligned} \text{Cutting Temperature (Ct)} = & -22.429+5.115A \\ & +2229.582B+140.271C-214.799D-13.750A* \\ & B+0.563A* C+0.981A * D-200.000 B * C-116.667 \\ & B * D+24.500 C * D-0.013 A^2+1441.967 B^2-89.235 \\ & C^2+21.691 D^2 \end{aligned} \quad (2)$$

From the mathematical model presented in equation (2), It can be deduced that the main variables influencing the cutting temperature were the speed, feed rate, depth of cut, and weight percentage of nanoparticles. Moreover, secondary components (i.e.) products of primary parameters were also acknowledged as significant

terms. The square terms are products of the squares of the primary parameters mentioned above. These indicate clearly that the quadratic terms of response present in the model.

The cutting speed (6.08), cutting feed (1.74), axial depth of cut (8.4), and concentration of alumina (14.32) are the statistical analysis values observed for surface roughness. The analysis also mentions that speed (8.18%), feed rate (2.34%) and depth of cut influences the roughness in the mentioned order.

The F-values showed that, in comparison to all other cutting factors, the concentration of nanoparticles of alumina had the greatest influence on surface roughness. The contribution percentages of speed, feedrate, depth of cut and wt% concentration are, 11.3% and 19.27% respectively.

The surface roughness R² score of 92% indicates a strong correlation between the cutting conditions predicted by the experiment and the actual ones. Morer R² indicates that the model is more accurate. The minimal error occurrence of the expected analysis is displayed in the predicted vs experimental figures.

$$\begin{aligned} \text{Surface roughness (R}_a\text{)} = & +1.218+0.0257A-12.448 \\ & B-0.975 C+0.103D-0.135 A * B+0.003 A * C \\ & -0.001A * D+2.250 B * C-1.583 B * D+0.050 C \\ & * D-0.001 A^2+93.268 B^2+0.223 C^2-0.059 D^2 \end{aligned} \quad (3)$$

It may be inferred indirectly from the ANOVA and

Table 8. ANOVA results for Surface Roughness (SR).

Source	SS	Dof	MS	F-value	p-value	Significant Level	% of Contribution
Model	1.13	14	0.0808	5.31	0.0248	Significant	100
A-Cutting speed	0.0924	1	0.0924	6.08	0.0488		8.18
B-Cutting feed	0.0264	1	0.0264	1.74	0.2353		2.34
C-Axial depth of cut	0.1277	1	0.1277	8.4	0.0274		11.30
D-Nanoparticles Al ₂ O ₃ concentration	0.2178	1	0.2178	14.32	0.0091		19.27
AB	0.169	1	0.169	11.11	0.0157		14.96
AC	0.0338	1	0.0338	2.22	0.1866		2.99
AD	0.0036	1	0.0036	0.2374	0.6434		0.32
BC	0.0364	1	0.0364	2.4	0.1726		3.22
BD	0.0144	1	0.0144	0.9494	0.3675		1.27
CD	0.005	1	0.005	0.3288	0.5872		0.44
A ²	0.0227	1	0.0227	1.49	0.2679		2.01
B ²	0.2878	1	0.2878	18.92	0.0048		25.47
C ²	0.0079	1	0.0079	0.522	0.4972		0.70
D ²	0.009	1	0.009	0.589	0.4719		0.80
Residual	0.0913	6	0.0152				
Lack of Fit	0.029	2	0.0145	0.9304	0.4658	not significant	
Pure Error	0.0623	4	0.0156				
Cor Total	1.22	20					

mathematical model that the major inputs i.e. speed, feed rate, depth of cut, and weight percentage of nanoparticle concentrations were expressing the substantial influence on surface roughness. Then, the alternate components like the products of speed, feedrate and depth of cut and wt% of nano particles concentration with each other also acknowledged as significant conditions. The square terms products of square of speed, feedrate and depth of cut and wt% of nano particles concentration are present in the Equation (3). These indicate clearly that the quadratic terms of response present in the model.

The equation demonstrated that surface imperfections diminish with increasing machining speed, with an increase in the weight percentage of nanoparticles having the greatest influence. This is followed by depth of cut and minor feed rate. The removal chip grains between work material and tool tip interface reduces the roughness. The friction at the cutting point is minimized by the creation of mist causes rolling larger nano particles like ball bearing effect. Due to huge spray pressure the chips were removed. Thus the reason initiates to reduce the roughness in marching area. Due to the interaction terms in the model, it was shown that roughness increased as the weight percentage of nanoparticles in the sample increased.

The results reveal that the regression model shows 92% variation in material roughness and 97% cutting temperature. The intention of analyzing the effect of cutting flow rate, wt% of nano particles concentration, Spindle speed, axial feed and DoC on roughness of the material and temperature of cutting zone is satisfied by ANOVA.

Result and Discussion

Interactive Plot effects on temperature in cutting zone

The surface reaction to the interaction curve that integrates with speed and cutting feed is plotted in three dimensions in Fig. 6. This illustrates the observed relationship between the cutting tool temperature and

machining speed and feed rate increases. The value of the machined surface decreases as the cutting temperature increases. This was mostly due to the fact that friction between the workpiece and the tool rises with increasing speed and feed rate. Higher cutting temperatures are the result of increased friction. The feed and cutting speed have a direct impact on the depth of cut. This affects both the temperature at the tool-chip interface and the rate of material removal as the depth of cut increases. The workpiece-cutting tool interface is under stress, which is causing the temperature to rise. The interaction diagram also shows that the cutting temperature increases with increasing alumina addition. This is due to the low heat dissipation of the titanium alloy, which causes poor thermal conductivity. Through the cutting fluids, a higher percentage of aluminum oxide by mass increases the cutting temperature and increases the thermal conductivity. In addition, the absence of alumina was found to decrease the performance of the cutting fluid, as the nanofluid has better wetting properties in the machining zone and between the sliding surfaces. This could be advantageous in two ways. Firstly, the coefficient of friction at the tool-part interface during machining might have been decreased due to the sliding actions of the nanoparticles.

Figure 6 shows how using a cutting fluid with nano-sized alumina diffusion can significantly lower the cutting temperature. When coolant is applied, a lubricating film forms at the intersection, lowering cutting temperatures and friction. This causes the temperature to drop. Because the layer between tool contacts in nanofluids was more stable and robust than in microfluids, lower temperatures have been reported while employing nanofluids. According to the interaction figures, the alumina-based nanofluid has a stronger cooling effect than regular fluids. This could be because the alumina-based nanofluid can accelerate the formation of films at higher temperatures, which boosts the fluid's heat transfer efficiency.

Interactive effects on surface roughness

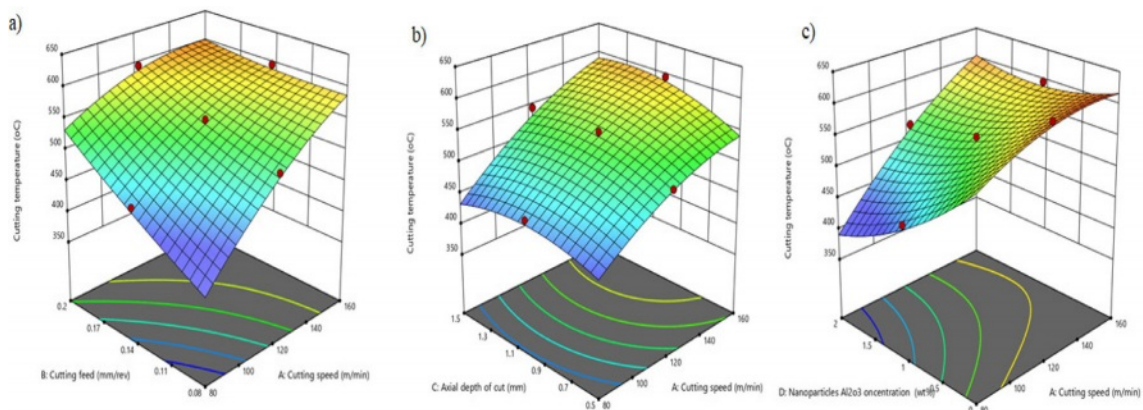


Fig. 6. Interactive plot for cutting temperature.

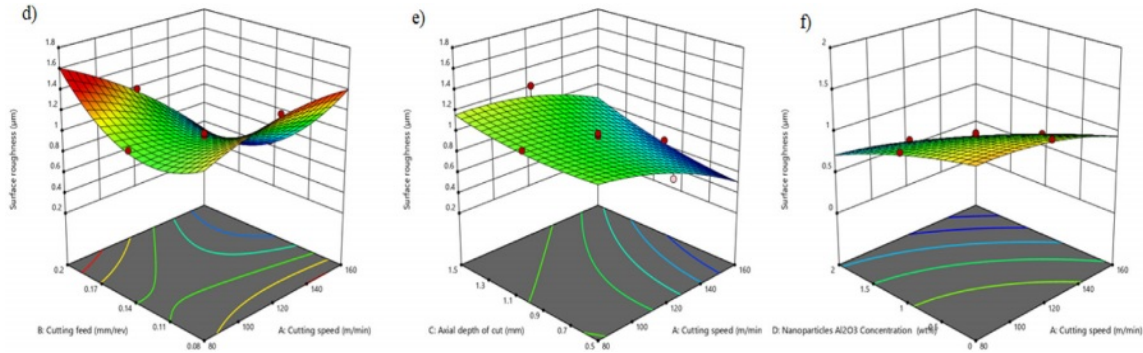


Fig. 7. Interactive plot for surface roughness.

Figure 7 illustrates how the parameters interact to determine the Ti-6Al-4V alloy's surface roughness. When a standard cutting fluid is used without alumina diffusion, the alloy's surface roughness values increase; this could be because the machining operation raised the temperature of the cutting tool. Lower cutting speed and feed led to poor machined surface quality and increased tool wear, as was evident from the interaction effects of machining parameters on surface integrity [35]. This was because a higher feed rate would overload the contact between the part and the tool, lowering the quality of the surface finish. The rougher the material surface is, the deeper the cut; this could be because the deeper cut creates tension when the topmost material is removed, which raises the cutting forces [36]. In 2% of alumina diffused cutting fluids, the lubricating capacity of coolant, when utilized in conjunction with alumina processing, has been measured in comparison to alumina without diffusion and a lower Ra value. A low Ra value has been noted in Fig. 7 as a result of improved lubrication and strong heat dispersion throughout the rake's face and side under dispersed alumina cutting fluids. During the machining process, the surface finish of Ti6Al4V alloy having less than 2% diffused alumina cutting fluids was superior to that of regular cutting fluids.

DFA based Multi objective optimization

Desirability function analysis (DFA) is indeed a valuable tool for optimizing process parameters, including those of nano-based cutting fluids, in machining processes. DFA identifies specific criteria or responses that reflect the desired outcomes of the process. These criteria may include, for example, surface finish, tool wear, cutting force, dimensional accuracy, and temperature rise during machining. For each criterion, a desirability function is defined that quantifies how desirable a certain level of that criterion is. One of the methods that is often utilized in the industry to increase response is the DFA. Three types of desirability functions are consistent with response characteristics: larger-the-better, nominal-the-better, and smaller-the-better [37]. During the numerical optimization stage, we employed the Design Expert-12 software package to lower the temperature and surface

roughness in order to determine the ideal speed, feed, axial depth of cut, and weight percentage concentration of alumina nanoparticles for milling Ti6Al4V alloy. For this investigation, every variable was made to fluctuate by minimizing the values of cutting temperature and surface roughness. The best options are reportable to reduce desirable value, as shown in Tables 8. The original task of DFA was to convert the response to a desired value between 0 and 1. If the value of the response variable is outside the acceptable range, it is marked as zero; if it is in its range, it is perceived as one.

Validation of Experiment

The desirability value around one validates the optimal settings that were chosen. Following numerous confirmation experiments, the determinant values were reported. once the optimal parameters for the principal values were found inside Table 9. The selected desirability levels and best practices for temperature and roughness in the Ti6Al4V milling process are displayed in Fig. 8. For Al₂O₃ fluid, the general desirability was 0.999. As a result, the overall desirability value is close to 1. DFA is a central and widely used method in multi-objective optimization design applications. This approach transforms the specified performance attributes of each expected response into a desired dimensionless value. The function's values fall between 0 and 1. The more favorable the next reaction is, the higher the value of d_i . The smallest, highest-quality feature was chosen for this investigation in order to change the surface roughness value. Thus, the equation is selected. The i -th answer y_i 's goal value is represented as T , the weight as W , the acceptable value's upper bound as U , and its acceptable value's lower bound as L response.

$$d_i = \begin{cases} 1 & y_i < T \\ \left(\frac{U-y_i}{U-T}\right)^w & T \leq y_i \leq U \\ 0 & y_i > U \end{cases} \quad (4)$$

It is possible to machine the Ti6Al4V alloy with the lowest cutting temperature and lowest surface roughness

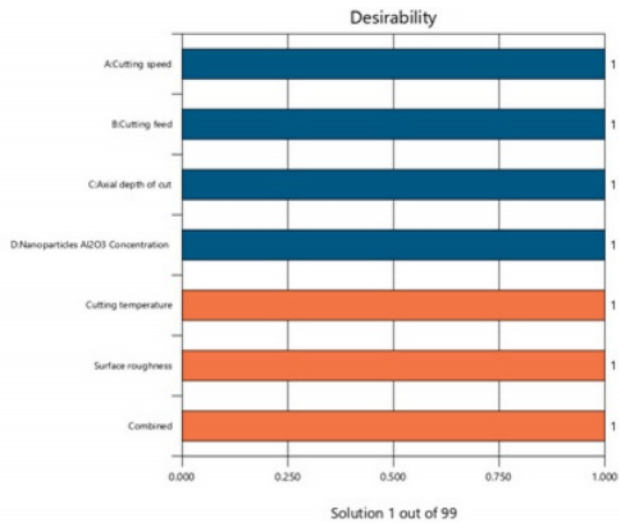


Fig. 8. DFA Solutions bar graph.

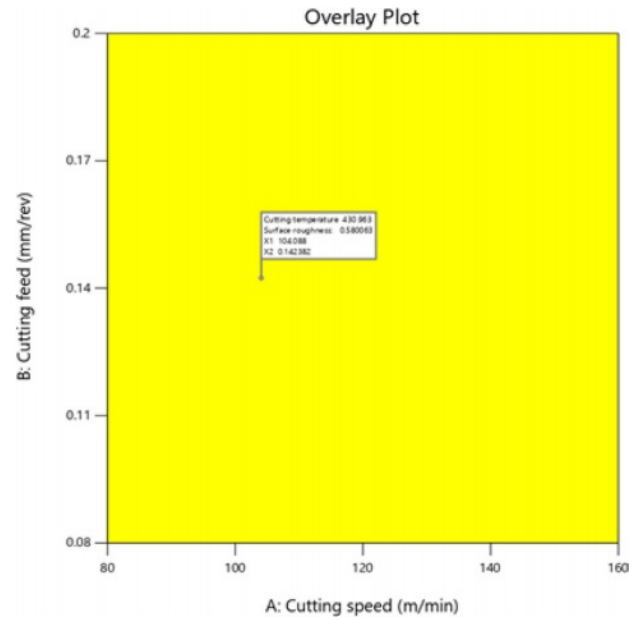


Fig. 9. DFA Solutions overlay plot.

by carefully adjusting the milling parameters. In order to maximize the lowest surface roughness and the smallest cutting temperature, consideration was given to each parameter’s variation gap, cutting situation, and relevance. Table 10 displays the conditions that were applied to the desirability function analysis. The desirability bar graph (Fig. 8) depicts the desirability for individual and combined effects for the responses. The ramp graph (Fig. 10) dot indicates the clear picture about the prediction of the output to the input.

The weight of Ct was three times as important as the weight of Ra, which was five times as important. According to an analysis of the overlay plot Fig. 9, the ideal cutting conditions are attained at A=104.0 m/min, B=0.142 mm/rev, C=0, 5 mm, and D=2. Consequently, the reactions were anticipated to have a desired value of

D=1 and a minimum value of "Ct" equal to 430.963°C and Ra=0.580 μm. Furthermore, the anticipated outcomes were confirmed, revealing that the anticipated values for surface roughness and cutting temperature were less than 3.6% and 2.8%, respectively.

Poor surface finish may result from the inappropriate selection of cutting fluid and cutting circumstances, which compromises surface integrity [38, 39]. The structure of the nanoparticles is crucial in enhancing the efficacy of the nanofluids. Because of the synergistic effect of alumina-based nanoparticles, liquid tribo-film production of nano-cutting fluid between the smooth surfaces increases the efficiency of nanofluids and decreases the coefficient of

Table 9. Desirability optimum solutions.

No	Spindle Speed	Feed rate	DoC	Al ₂ O ₃ – Nano Nanoparticles Cconcentration	Temperature	Surface roughness	Desirability
1	104.088	0.142	0.5	2	430.963	0.58	1
2	103.87	0.143	0.5	2	430.994	0.58	1
3	104.662	0.141	0.5	2	431.037	0.58	1

Table 10. DFA applied conditions.

Milling parameters	Goal	Lower	Upper	Lower	Upper	Importance
Speed	Limit	80	160	1	1	3
Feed	Limit	0.08	0.2	1	1	3
DoC	Limit	0.5	1.5	1	1	3
Al ₂ O ₃ nano - concentration	Limit	0.0	2.0	1	1	3
Cutting temperature	minimum	431	626	1	1	3
Roughness	minimum	0.58	1.43	1	1	5

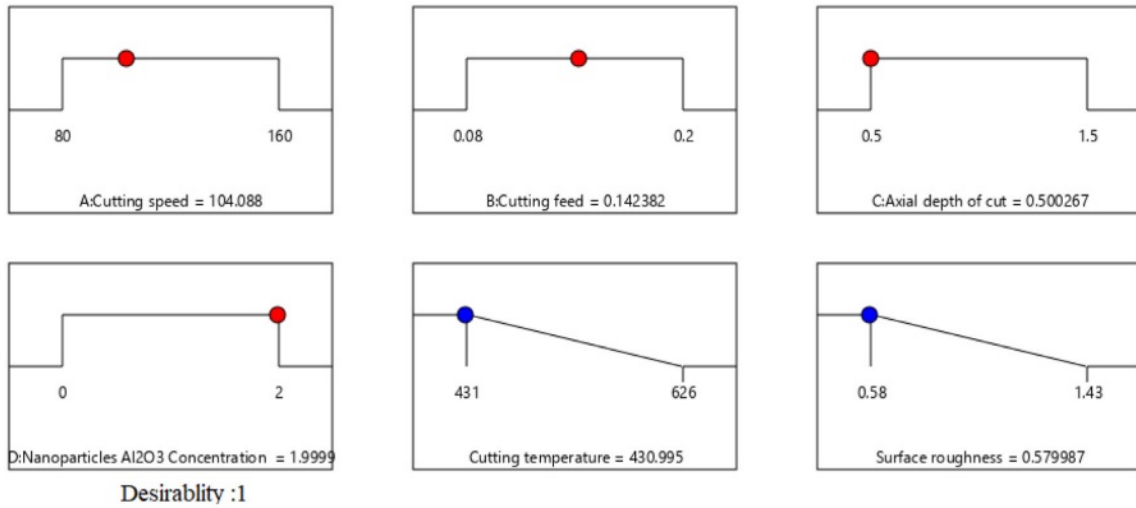


Fig. 10. Ramp graphs of optimized and predicted values.

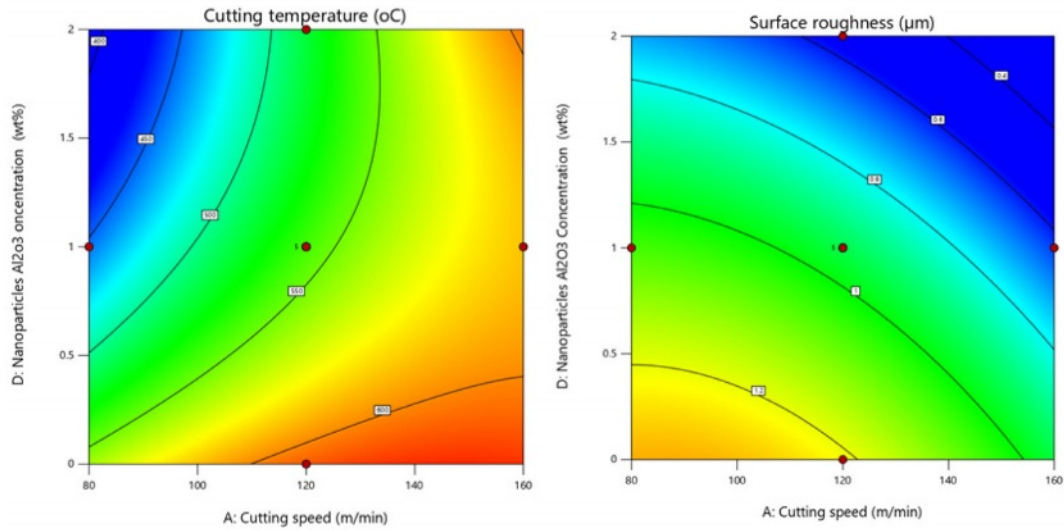


Fig. 11. Performance measure of Ct and Ra.

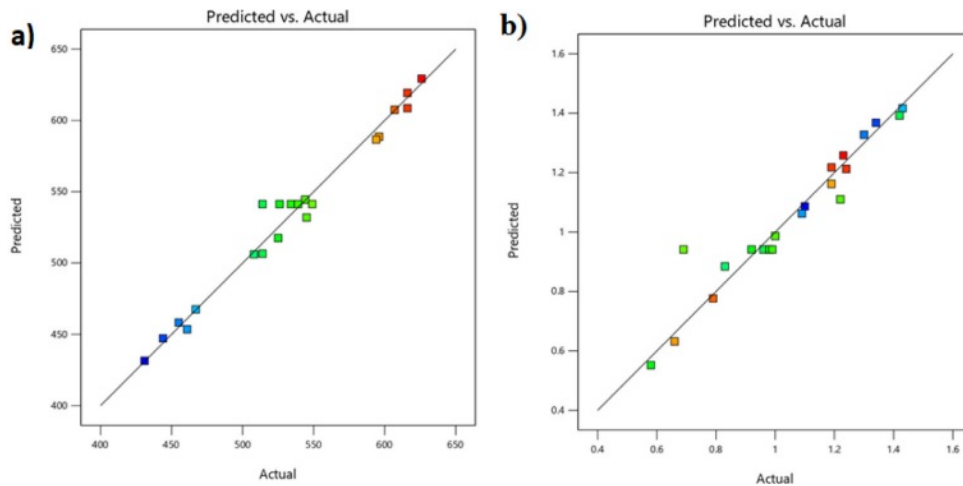


Fig. 12. predicted Vs actual value for cutting temperature and surface roughness.

friction [40, 41]. Additionally, as Fig. 11 illustrates, the wettability of nanofluids was improved by the mixer of mildly cutting fluids based on alumina. Reasons for the differences may be due to differences in particle cluster size, differences in dispersion techniques, and the use of a surfactant similar to that previously reported in thermal conductivity data. At lower concentrations, the change in relative viscosity with temperature was minimal [42].

The cutting zone's temperature (97%) and surface roughness (92%) demonstrate the strong correlation between the cutting conditions anticipated by experiment and those observed in practice. Fig. 12 illustrates the minimum error occurrence of the anticipated analysis for satisfactory validation, comparing it with the experimental data.

Conclusion

A nano-alumina-based cutting fluid was used during the Ti-6Al-4V machining process to study its effect on surface roughness and cutting temperature. The conclusions of the study were as follows:

1. The roughness and decrease in cutting temperature were affected by the addition percentage of nano-alumina-based cutting fluid.
2. There was good agreement between the experimental and anticipated machining conditions and the R² values for the responses, such as 92% and 97% for roughness and cutting temperature, respectively.
3. Compared to tests carried out without nano-additives, the use of nano-alumina-based cutting fluid results in superior surface roughness and cutting temperature.
4. At 2% alumina diffused cutting fluids, the lubricity of the coolant used in alumina machining was compared to no alumina diffusion, a lower cutting temperature, and surface roughness values.
5. The best machining performance is demonstrated by the multi-target optimization results when the ideal cutting circumstances (A=104.0 m/min, B=0.142 mm/rev, C=0.5 mm, and D=2) are chosen. With a minimum Ct value of 430.995°C and Ra=0.579 μm at the intended value of D=1.
6. The output showed the expected reactions and the projected values for cutting temperature, surface roughness and desirability were 430.995°C, 0.58 μm and D=1 respectively.
7. Future studies should concentrate on the impacts of nano additive concentration and the size of the nanofluid with various soft particles that serve as reinforcement.

Future study

1. Machine learning techniques can be used to develop intelligent algorithms that use simple computational methods to solve many optimization problems.
2. Computer modeling helps to investigate fluid

dynamics, heat transfer and material deformation during machining, and to show what different phenomena affect the machining process.

3. It is important to verify the effectiveness of the proposed approach in an engineering environment. Further research will focus on expanding the use of nanocutting fluids in industrial environments, taking into account factors such as cost-effectiveness, compatibility with existing equipment and legal compliance.
4. It is important to assess the environmental and health impacts of nanocutting fluids throughout their life cycle to ensure their safe and sustainable use. Further research may develop methods to assess the risks associated with exposure to nanoparticles and strategies to reduce environmental contamination and occupational hazards.

Declaration

There is no conflict from authors and there no fund received from any agency for this experimental work.

References

1. R. Banerjee, S. Nag, and H.L. Fraser, *Mater. Sci. and Eng:C* 25[3] (2005) 282-289.
2. C.R. Dandekar, Y.C. Shin, and J. Barnes, *Int. J. Mach. Tool. Manu.* 50[2] (2010) 174-182.
3. A. Bhattacharyya in "Metal Cutting: Theory and Practice" (New Central Book Agency (P) Ltd, Calcutta, 1984) p.21-32.
4. C.H. Che-Haron and A. Jawaid, *J. Mater. Process. Technol.* 166[2] (2005) 188-192.
5. C. Chanakyan and S. Sivakumar, *J. Ceram. Process. Res.* 21[6] (2020) 647-655.
6. A. Shokrani, V. Dhokia, and S. T. Newman, *J. Manuf. Process.* 21 (2016) 172-179.
7. K. Aslantas and A. Cicek, in proceeding of the 8th CIRP Conference on High Performance Cutting, 2018, edited by László Monostori, Gabor Stepan and Dániel Bachrathy, (*Procedia CIRP* 2018) 77 (2018) p.70-73.
8. G.K.M. Rao, R. Padmini, and P.V. Krishna, *Tribology International* 94[1] (2016) 490-501.
9. H. Hegab, U. Umer, M. Soliman, and H.A. Kishawy, *Int. J. Adv. Manuf. Technol.* 96[1-10] (2018) 3449-3458.
10. P. Mutharasu and M. Kathiresan, *J. Ceram. Process. Res.* 22[6] (2021) 697-704.
11. R.S. Revuru, J.Z. Zhang, N.R. Posinasetti, and T. Kidd, *Int. J. Adv. Manuf. Technol.* 95[1-4] (2018) 1451-1463.
12. M. Srinivasan, S. Ramesh, S. Sundaram, and R. Viswanathan, *J. Ceram. Process. Res.* 22[3] (2021) 345-355.
13. A.K. Sharma, A.K. Tiwari, and A.R. Dixit, *J. Cleaner Prod.* 127 (2016) 1-18.
14. H. Hegab, H.A. Kishaway, M.H. Gadallah, U. Umer, and I. Deiab, *Int. J. Adv. Manuf. Technol.* 97[5-8] (2018) 1593-1603.
15. K.M.S. Kumar, T. Ramanathan, S. Murugasan, and V. Thangamuthu, *J. Ceram. Process. Res.* 22[6] (2021) 731-738
16. M. Usha and G.S. Rao, *Tribol. Ind.* 44[1] (2022) 1-15.
17. S.H. Ahn and K.W. Nam, *J. Ceram. Process. Res.* 18[11]

- (2017) 767-776.
18. S. Khandekar, M. Ravishankar, V. Agnihotri, and J. Ramkumar, *Mater. Manuf. Process* 27 (2012) 1-5.
 19. T. Siva and K. Anandavelu, *J. Ceram. Process. Res.* 24[2] (2023) 406-414.
 20. P. Bagyalakshmi, P.A. Varthanan, and P.D. Randheer, *J. Ceram. Process. Res.* 23[3] (2022) 356-366.
 21. E. Abdelkrem, N. Ibrahim, and D. Ibrahim, *J. Manuf. Mater. Process.* 5 (2021) 42.
 22. I. Sharmain, M.A. Gafur, and N.R. Dhar, *SN Applied Sciences*, Springer Nature [2] (2020) 626.
 23. B.S. Babu, G. Chandramohan, C. Boopathi, T. Prithar, and R. Srinivasan, *J. Ceram. Process. Res.* 19[1] (2018) 69-74.
 24. I.A. Choudhury and M.E. Baradie, *J. Mater. Process Tech.* 95[1] (1999) 30-39.
 25. M. Changmai, J.P. Priyesh, and M.K. Purkait, *J. Sci.: Adv. Mater. Devices* 2[4] (2017) 483-492.
 26. B. Rahmatinejad, *J. Nanostruct.* 12[3] (2022) 642-659.
 27. F. Gagan, T. Kivak, C.V. Yildirim, and M. Sarikaya, *J. Mater. Res. Technol.* 9[5] (2020) 10386-10400.
 28. R. Kumar, A.K. Sahoo, P.C. Mishra, and R.K. Das, *Int. J. adv. Manuf. Technol.* Online publication, 2019.
 29. C. Manivel and L. Savadamuthu, *Digest J. Nanomater. Biostruct.* 15[3] (2020) 809-814.
 30. K.K. Gajrani, P.S. Suvin, S.V. Kailas, and M.R. Sankar, *J. Mater. Process. Technol.* 266 (2019) 125-139.
 31. D.G. Subhedar, Y.S. Patel, B.M. Ramani, and G.S. Patange, *Clean. Eng. Technol.* 3 (2021) 100104.
 32. A. Mamedov and I. Lazoglu, *J. Mater. Process. Technol.* 229 (2016) 659-667.
 33. Douglas C. Montgomery in "Design and Analysis of Experiments" 6th Edition (John Wiley & sons, New York, 2005) p.757.
 34. N.K. Sahu and A.B. Andhare, *J. Comput. Des. Eng.* 6[1] (2019) 1-12.
 35. W. Gary and Oehlert in "A first course in design and Analysis of Experiments", (W.H. Freeman, 2000) p.679.
 36. B. Gep and D.W. Behnken, *Technometrics* 2 (1960) 455-475.
 37. H. Oktem, T. Erzurumulu, and H. Kurtaran, *J. Mater. Process. Technol.* 170 (2005) 11-16.
 38. D. Yang and Z. Liu, *Int. J. Refract. Met. Hard Mater.* 51 (2015) 192-200.
 39. K.M.S. Kumar, T. Ramanathan, S. Murugasan, and V. Thangamuthu, *J. Ceram. Process. Res.* 22[6] (2021) 731-738.
 40. A.K. Parida and K. Maity, *Measurement* 137 (2019) 375-381.
 41. Coello Carlos A. Coello and Gary B. Lamont in "Applications of multi-objective evolutionary algorithms" (Published by World Scientific 2004, V1) p.29.
 42. L. Senthilkumar, L. Savadamuthu, and C. Manivel, *J. Ceram. Process. Res* 23[4] (2022) 476-489.